JOURNAL OF MATERIALS SCIENCE 32 (1997) 3995–4003

Oxidized potato-starch films as primer coatings of aluminium

T. SUGAMA
Energy Efficiency and Conservation Division, Department of Applied Science, Brookhaven National Laboratory, Upton, NY 11973, USA

Potato-starch (PS) films for use as primer coatings of aluminium substrates were prepared in two steps, chemical–thermal–catalysed oxidation routes. The PS was modified with cerium (IV) ammonium nitrate (CAN) as a chemical oxidizer, followed by thermal oxidation at 150 °C in the presence of atmospheric oxygen; this led to the formation of a functional carbonyl derivative caused by cleavage of the glycol C–C bonds in glycosidic rings, thereby resulting in the ring openings. Increasing oxidation by raising the temperature to 200 and 250 °C promoted the conversion of carbonyl into carboxylate derivatives, while facilitating the breakage of C–O–C linkages in the open rings. The latter phenomenon reflected the formation of another carboxylate. The intermediate carboxylate derivatives favourably reacted with Ce^{4+} ions released from CAN to form cerium-bridged carboxylate complexes. Cerium-complexed carboxylate films used as primer coatings not only afforded some protection of aluminium substrates against corrosion, but also displayed excellent adhesion to both the polyurethane (PU) top-coating and aluminium sites. The latter demonstrated that the loss of adhesion at PU/primer/aluminium joints occurs in the PU layers, representing the mode of cohesive failure.

1. Introduction

Current and pending environmental, health and occupational safety regulations impose serious constraints on industries producing corrosion-protective coatings. One such example is the requirement that all paints containing $>250\ g\,l^{-1}$ volatile organic compound (VOC) emissions are removed from the market. In addition, chromium and lead compounds are environmentally hazardous, and there is growing pressure to eliminate their use in corrosion barriers for metals and as fillers and pigments in paints [1]. Particular attention is being paid to the large amount of hexavalent chromium as hazardous waste generated from chromium-conversion coating technologies which are commonly used as corrosion protection of anodized aluminium alloys. As a result, effective, environmentally benign material systems are needed as corrosion-protective coatings on metals.

In an attempt to mitigate such environmental impacts, our emphasis has focused on the usefulness of environmentally benign natural polymers, such as pectin and starch, as water-based coating systems to protect de-anodized aluminium from corrosion. Regarding the natural polymers, worldwide, a 1985 survey on the consumption of starch as a natural polymer indicated a total usage of $\approx 1700 \times 10^6$ ton y^{-1} [2]. By the year 2000, its products are estimated to reach about 2000×10^6 tons. Because the source of starch comes from the seeds and roots of plants as renewable agricultural resources, it is abundant, comparatively inexpensive, and relatively stable in quality and price. Thus, using starch as an extender and replacement for synthetic polymers might reduce our dependence on petrochemical-derived products. However, the direct use of natural polymers as protective coatings without any molecular modifications has three undesirable problems: (1) the settlement and growth of microorganisms in its aqueous solutions, (2) the high susceptibility of films to moisture, and (3) the poor chemical affinity of natural polymers for aluminium surfaces.

We succeeded in overcoming these drawbacks by grafting polyorganosiloxane (POS) polymers on to the natural polymer chains [3]. Such graftings were attained through heat-catalysed dehydrating polycondensation reactions between the OH or COOH groups in natural polymers and the silanol end groups in POS.

On the other hand, as already reported by several investigators [4–6], the graft copolymerization of vinyl monomers, such as acrylonitrile and methyl methacrylate, on to starch, can be initiated by cerium (IV) and manganese (III) salts as oxidizing agents. Specifically, these agents not only incorporated oxygen-based functional derivatives, such as aldehydic, ketonic, and carboxyl groups, into the starch, but also contributed to converting these functional derivatives in the oxidized starch into enolic groups. Finally, the reaction between enols and Ce^{4+} or Mn^{3+} led to the generation of free radicals caused by the opening of glycosidic rings in the starch, thereby propagating the rate of radical polymerization in assembling the grafting conformation of vinyl polymers on to the starch.

0022–2461

From this information, our particular interest was to investigate the role of the oxygen-based functional derivatives formed in the oxidized starch polymers without any grafted conformation, in applications as primer coatings of aluminium substrates. The combined techniques of chemical and thermal oxidations were employed to promote the rate of oxidation of starch polymers; namely, in the former process Ce (IV) salt was used as the chemical oxidizing agent, while the latter was accomplished by heating them in the presence of atmospheric oxygen at elevated temperatures.

Attention was paid to the characteristics of the oxidized starch coatings in protecting aluminium from corrosion and in adhering to the polyurethane top-coatings. To obtain this information, our studies included the changes in molecular conformation of starch polymers as a function of oxidation, the rate of electrolyte penetration passing through the coating film for evaluating its ability to prevent corrosion of aluminium, its salt-spray resistance, and the chemistry at interfaces between the oxidized starch primer and the polyurethane or aluminium to understand its adherence behaviour.

2. Experimental procedure

2.1. Materials

The starch used was potato starch (PS) from ICN Biomedical, Inc. Cerium (IV) ammonium nitrate [$(Ce(NH_4)_2(NO_3)_6$] (CAN), supplied from Alfa, was used as the oxidizing agent. Chemical oxidation of a 1.0 wt % PS colloidal solution dissolved in deionized water at 80 °C was achieved by adding CAN at 0.03%, 0.07%, 0.15% and 0.30% by weight of the total PS solution. The lightweight metal substrate was a 6061-T6 aluminium sheet containing the following chemical constituents: 96.3 wt % Al, 0.6 wt % Si, 0.7 wt % Fe, 0.3 wt % Cu, 0.2 wt % Mn, 1.0 wt % Mg, 0.2 wt % Cr, 0.3 wt % Zn, 0.2 wt % Ti, and 0.2 wt % other elements. Commercial-grade polyurethane (PU) M313 resin, supplied by the Lord Corporation, was applied as an elastomeric top-coating. The PU was polymerized by incorporating a 50% aromatic amine curing agent, M201. The topcoat system was then cured in an oven at 80 °C.

2.2. Coating technology

The aluminium surfaces were coated by CAN-modified and unmodified PS films in the following sequence. As a first step to remove surface contaminants, the aluminium substrates were immersed for 20 min at 80 °C in an alkaline solution consisting of 0.4 wt % NaOH, 2.8 wt % tetrasodium pyrophosphate, 2.8 wt % sodium bicarbonate, and 94.0 wt % water. The alkali-cleaned aluminium surfaces were washed with deionized water at 25 °C for 5 min, and dried for 15 min at 100 °C. Then, the substrates were dipped into a soaking bath of solution at room temperature, and withdrawn slowly. The wetted substrates were then heated in an oven for 120 min at 150, 200 and 250 °C, to yield thin solid films. Also, this heating process promoted the rate of thermal oxidation of the films.

2.3. Measurements

To understand the changes in molecular structure of CAN-modified and unmodified PS as a function of temperature, discs for Fourier transform–infrared (FT–IR) analysis were prepared by mixing 200 mg KBr and 2–3 mg powdered PS sample that had been granulated to a size of < 0.074 mm. An X-ray photoelectron spectroscopy (XPS) study on the surfaces of these PS films was carried out to support the FT–IR data. XPS was also used to identify the locus of failure at the PU/PS/Al joints. The thickness of films deposited to the aluminium was determined by a surface-profile measuring system.

A.C. electrochemical impedance spectroscopy (EIS) was used to evaluate the ability of the coating films to protect aluminium from corrosion. The specimens were mounted in a holder, and then inserted into an electrochemical cell. Computer programs were prepared to calculate theoretical impedance spectra and to analyse the experimental data. Specimens with a surface area of 13 cm^2 were exposed to an aerated 0.5 N NaCl electrolyte at 25 °C, and single-sine technology with an input a.c. voltage of 10 mV (r.m.s.) was used over a frequency range of 10 kHz to 10^{-2} Hz. To estimate the protective performance of coatings, the pore resistance, R_{po}, was determined from the plateau in Bode-plot scans (impedance (Ωcm^2) versus frequency (Hz)) that occurred at low-frequency regions. The salt-spray tests of unmodified and modified PS-coated aluminium panels (75 mm × 75 mm, size) were performed in accordance with ASTM B 117, using a 5% NaCl solution at 35 °C.

3. Results and discussion

3.1. Oxidation of PS

Fig. 1 shows the FT–IR absorption spectra of the unmodified and 0.07, 0.15, and 0.3 wt % CAN-modified PS samples at 150 °C, over the frequency range of 4000–1000 cm^{-1}. For unmodified PS polymers, denoted as 0%, a typical spectrum enclosed absorption bands at 3420 cm^{-1}, revealing the O–H stretching vibration of OH groups in the glucose units, at 2930 cm^{-1}, and 1460 and 1370 cm^{-1} which can be ascribed to the C–H stretching and bending modes of the methylene, respectively, at 1640 cm^{-1}, originating from the bending vibration of H–O–H in the absorbed H_2O, and also at 1150, 1090, and 1020 cm^{-1}, reflecting the stretching mode of C–O–C linkages in the glucosidic rings. Similar spectral features were seen with the 0.07 wt % CAN-oxidized PS samples. Increasing the concentration of CAN to 0.15 and 0.3 wt % resulted in the appearance of a new absorption band at 1720 cm^{-1}, corresponding to the C=O groups, while the C–H bending mode at 1370 cm^{-1} somewhat shifted in frequency to a low wave number site at 1320 cm^{-1}. This information implied that a high rate of oxidation of PS polymers, induced by adding a certain amount of CAN, favourably

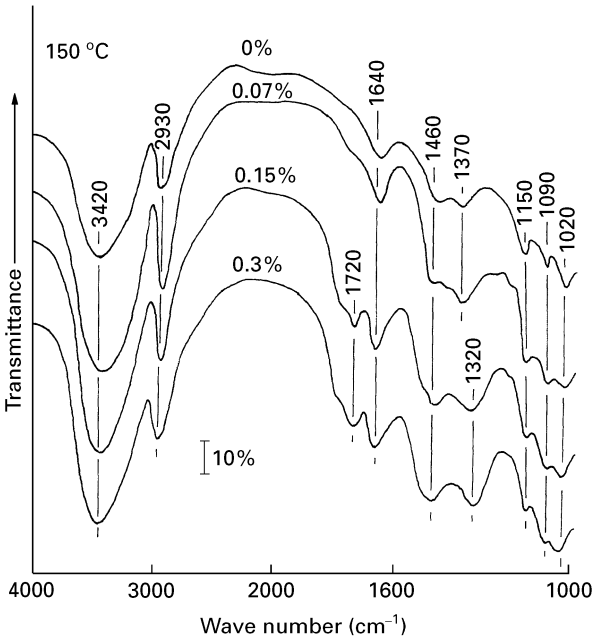

Figure 1 FT–IR absorption spectra of 0, 0.07, 0.15, and 0.3 wt % CAN-modified PS at 150 °C.

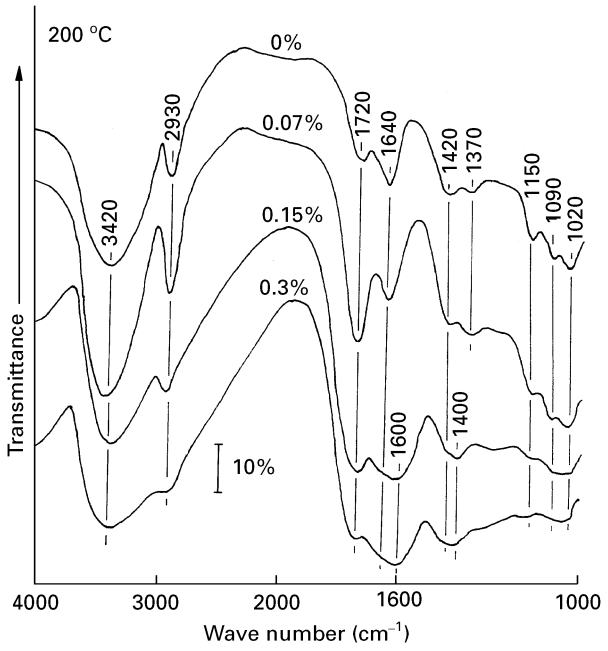

Figure 2 Comparison between IR spectral features of 0, 0.07, 0.15 and 0.3 wt % CAN-modified PS at 200 °C.

introduces the C=O groups into its molecular structure. Doba *et al.* [5] have reported that the C=O groups were formed by oxidation-caused cleavage of glycol C–C bond in the glycosidic rings. The subsequent opening of the rings caused by such cleavage not only led to the formation of C=O groups, but also generated free-radicals which promoted the rate of grafting of the vinyl monomer on to the PS. Fig. 2 depicts the FT–IR spectra of these samples treated at 200 °C. As is seen, although the CAN was unmodified, the spectrum of the bulk PS polymers was representative of the growth of C=O band at 1720 cm^{-1}. This finding clearly demonstrated that the incorporation of additional oxygens into the PS by thermal oxidation at 200 °C also provides the formation of C=O groups, corresponding to the opening of the rings by cleavaging the glycol C–C bond. As expected, PS modified with 0.07 wt % CAN revealed a further growth of the C=O band.

Next, attention centred on the spectral features of the 0.15 and 0.30 wt % CAN-modified PS samples which were quite different from those of the 0 and 0.07 wt % CAN samples: in particular, there was (1) a striking reduction in the intensity of the methylene-related bands at 2930, 1420 and 1370 cm^{-1}, and also of the C–O–C linkage-associated bands in the range 1120–1000 cm^{-1}, and (2) the emergence of strong new bands near 1600 and 1400 cm^{-1} frequencies, while the peak intensity of the C=O band became weaker. Regarding result 2, these new bands might be attributable to the formation of carboxylate groups in which the absorptions at 1600 and 1400 cm^{-1} are due to the asymmetric and symmetric stretching of COO^-, respectively [7]. If such assignments are correct, we assumed that the incorporation of more oxygens into the PS by the combination of chemical and thermal oxidations not only transforms the C=O into carboxylate groups, but also causes oxidation-induced breakage of C–O–C linkages, reflecting result 1,

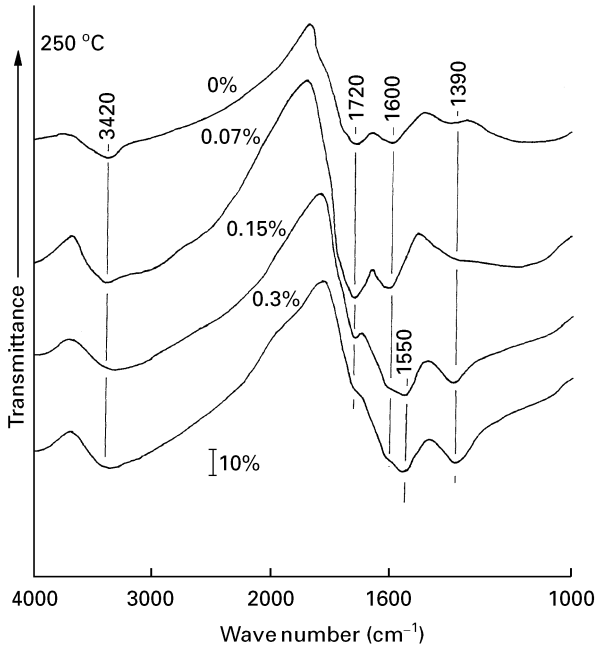

Figure 3 Changes in spectral features of 0, 0.07, 0.15 and 0.3 wt % CAN-modified PS at 250 °C.

thereby resulting in the decomposition of ring structures, and correspondingly, the removal of methylene groups from the PS. This breakage may also create C=O and carboxylate derivatives. A further increase in temperature to 250 °C enhanced the extent of the conversion of C=O into carboxylate. As shown in Fig. 3, although there was no modification with CAN, its spectrum had carboxylate bands at 1600 and 1390 cm^{-1}. With CAN-modified PS samples, the comparison between the spectral features clearly verified that the extent of peak intensity of the C=O band at 1720 cm^{-1} tends to reduce with an enhanced intensity of the carboxylate band in the range

1600–1550 cm^{-1}. Hence, the extent of C=O to carboxylate conversion seems to depend on the rate of oxidation of PS. Furthermore, a highly oxidized PS led to the decomposition of the ring structure because of the disappearance of the C–O–C linkage-associated bands ranging from 1150 to 1020 cm^{-1}, and reducing considerably the OH group-related band at 3420 cm^{-1}. As a result, it is possible to assume that the breakage of C–O–C linkages caused by incorporating an abundance of oxygen may serve in forming additional carboxylate derivatives.

This information was supported by identifying the chemical states of unmodified and 0.3 wt % CAN-modified PS film surfaces after exposing them for 2 h in air at 150 and 250 °C, by XPS. In XPS core-level spectra, the scale of the binding energy (BE) was calibrated with the C1s of the principal hydrocarbon-type carbon peak fixed at 285.0 eV as an internal reference standard. A curve deconvolution technique, using a Du Pont curve resolver, was employed to substantiate the information on the carbon-related chemical states from the spectrum of the carbon atom. For the unmodified PS samples (Fig. 4), the C1s spectrum at 150 °C had two resolvable Gaussian components at the BE positions of 285.0 and 286.5 eV, denoted as peak areas 1 and 2. The major peak at 285.0 eV is associated with the carbon in CH_2 and CH groups as the principal component. The secondary intensive peak at 286.5 eV originates from the carbon in $–CH_2O–$ (e.g. alcohol and ether). Noticeable changes in the shape of the C1s region were observed in the 250 °C treated samples. The spectrum was characterized by the excitation of two new signals at 288.3 and 289.6 eV, corresponding to peak areas 3 and 4, respectively, and also by a striking attenuation of the area 2 signal. The possible assignments of signals at 288.3 and 289.6 eV are due to the carbon in C=O and COO^- groups, respectively [8]. Assuming that the assignments of these peaks are correct, this information strongly supported the data obtained from the FT–IR studies; namely, the susceptibility of PS to oxidation at 250 °C led to the development of C=O and COO^- groups, while the elimination of the alcohol and ether groups from the rings was reflected in a striking decay of the peak area at 286.5 eV. In other words, both the alcohol and ether groups may be converted into C=O and carboxylate derivatives by oxidation. In contrast, a quite different overall curve structure was seen from modified PS film surfaces at 150 and 250 °C (Fig. 5). At 150 °C, the curve

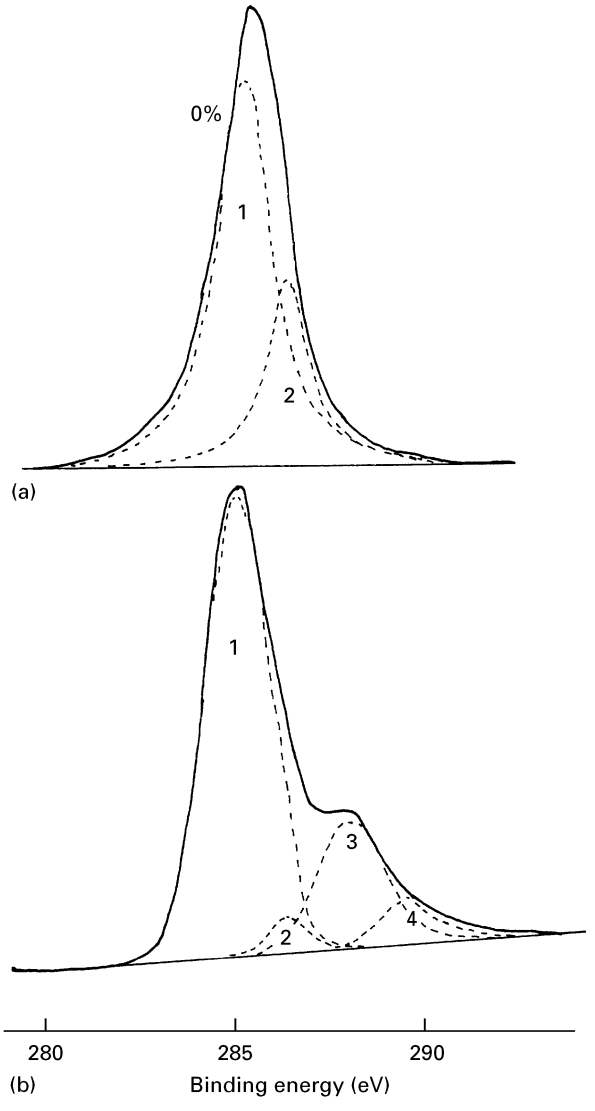

Figure 4 C1s core-level spectra for (a) 150 and (b) 250 °C oxidized bulk PS samples. 1, 285 eV; 2, 286.5 eV; 3, 288.3 eV; 4, 289.6 eV.

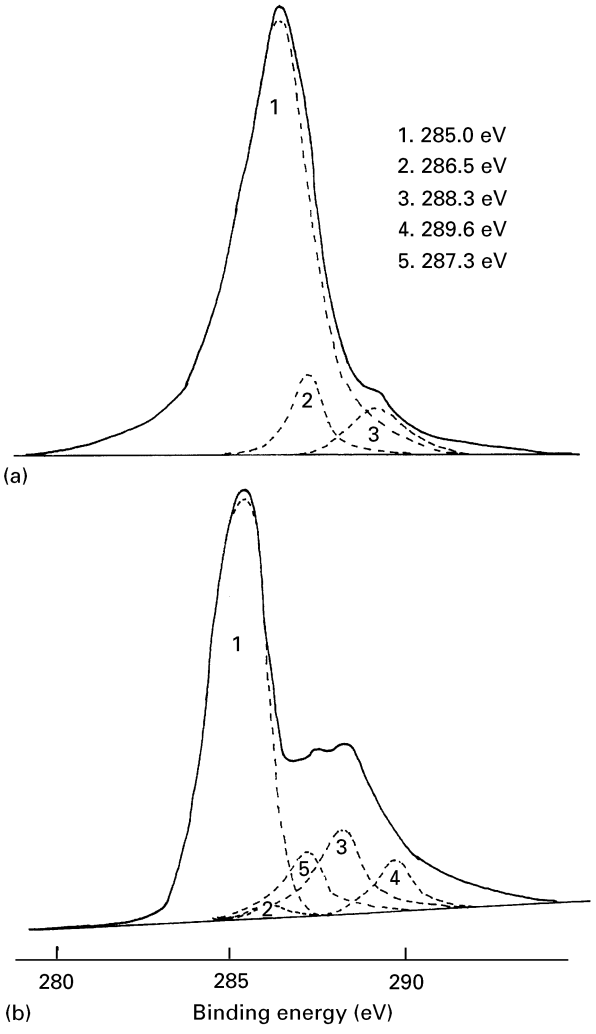

Figure 5 C1s region for 0.3 wt % CAN-modified PS samples at (a) 150 and (b) 250 °C. For key, see Fig. 4.

included the C=O related peak (area 3) at 288.3 eV, suggesting that even though the temperature of heat treatment was relatively low, adding CAN progressively promotes the rate of oxidation of PS to introduce C=O derivatives into the ring structure. A further promotion in oxidation by heating the samples to 250 °C resulted in an interesting spectral feature; namely, two new signals at 289.6 and 287.3 eV, belonging to areas 4 and 5. The former signal is assignable to the carbon in carboxylate groups. According to the literature [9], the contributor to the latter signal, which is located in BE positions between $-CH_2O-$ and C=O groups, may be due to the carbon in the metal-complexed carboxylate compounds. In this PS system, the only source of metal species comes from the CAN; it is cerium. Thus, the possible formulas of cerium complexed carboxylate are as follows

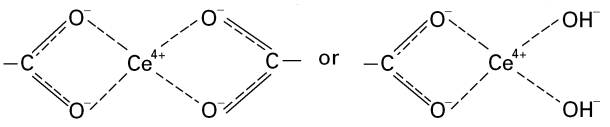

One formula is that in which Ce^{4+} ions released from CAN in an aqueous medium favourably complex with the carboxylate anions (COO^-) to form Ce^{4+} salt-bridge structures which link two adjacent carboxylates; the other formula represents a half-salt conformation containing two OH groups. Accordingly, such cerium-complexed carboxylates might be produced through the following oxidation pathways: first, the C=O derivatives are developed by preferential oxidation of glycol groups in the glycosidic rings by Ce^{4+} ions in the presence of atmospheric oxygen at low temperature; while the cleavage of the glycol C–C bond occurs followed by opening the ring. Second, enhancing the rate of oxidation by increasing the temperature not only leads to the conversion of C=O into carboxylate derivatives, but also causes the breakage of the C–O–C linkages in the ring. The latter phenomenon further promotes the formation of carboxylate because of the oxidation of alcohol and ether groups present in ring, thereby resulting in the decomposition of PS structure. Finally, the carboxylate anions (COO^-) favourably react with Ce^{4+} to form Ce^{4+} salt-bridge conformations which play an essential role in binding the COO^- ions.

The XPS study was extended to inspect the $Ce3d_{5/2}$ region of the 0.3 wt % CAN-modified PS film surfaces at 150 and 300 °C (Fig. 6). At 150 °C, the spectrum included two signals at 884.6 and 882.4 eV; the possible assignment of the latter signal is the cerium in the CeO_2 [10]. Although no information was found in the literature on surface sciences, the former signal may be due to the cerium in the cerium-complexed carboxylate compounds. Increasing the oxidizing temperature to 300 °C corresponded to a marked growth of the overall curve, suggesting that a large amount of the oxidized and complexed compounds was formed on the film's surfaces.

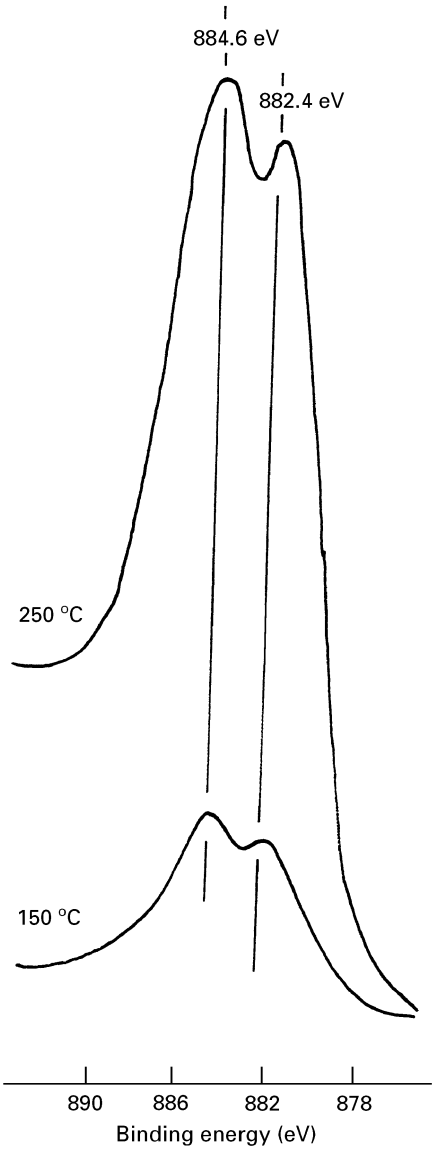

Figure 6 $Ce3d_{5/2}$ region for 0.3 wt % CAN-modified PS samples at 150 and 300 °C.

3.2. Corrosion protection

The research subject focused on investigating the ability of the oxidized PS coating films deposited on the aluminium substrate surfaces to protect them from corrosion. As described in Section 2, the coating films were prepared by dipping alkali-cleaned aluminium substrates into unmodified, and 0.07, 0.15, and 0.3 wt % CAN-modified PS solutions, followed by heating for 120 min in an air oven at 150, 200, and 250 °C. The thickness of films deposited on the aluminium ranged from $\approx$1.0 to $\approx$2.5 μm. Two corrosion-related tests, a.c. electrochemical impedance spectroscopy (EIS) and salt-spray resistance, were carried out to evaluate the effectiveness of coating films in reducing the rate of corrosion of aluminium.

In EIS examination, our attention focused on the impedance value of the element, $|Z|$, in the Bode-plot features (the absolute value of impedance, $|Z|$, $\Omega\,cm^2$, versus frequency, Hz); this value can be determined from the plateau in the Bode plot occurring at a frequency of 10^{-1} Hz for modified PS coatings, and at 10^0 Hz for unmodified PS and uncoated aluminium

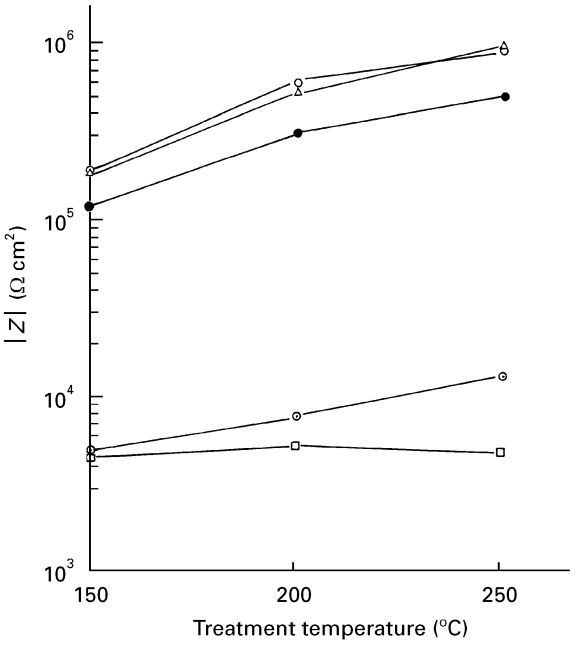

Figure 7 Changes in impedance, $|Z|$, values for CAN-modified and unmodified PS coatings as a function of thermal-oxidation temperature. (□) Aluminium substrate, modified with (⊙) 0%, (●) 0.07%, (△) 0.15% and (○) 0.30% CAN.

specimens. Fig. 7 shows the changes in $|Z|$ value as a function of thermal-oxidation temperature of the film. The impedance of the uncoated aluminium substrates treated at these temperatures ranged from $\approx 4.5 \times 10^3$ to $\approx 5.4 \times 10^3\ \Omega\text{cm}^2$. When the aluminium surfaces were coated with unmodified and CAN-modified PS films, the data demonstrated that the value of $|Z|$ depended mainly on two parameters, the concentration of CAN and the temperature; i.e. the increases in the concentration of CAN and treatment temperature reflected an increasing $|Z|$ value. Although the $|Z|$ value for the unmodified PS films gradually rises with an increase in temperature, the highest value at 250 °C was only $\approx 1.3 \times 10^4\ \Omega\text{cm}^2$. In contrast, all the CAN-modified coatings displayed an impedance of $> 10^5\ \Omega\text{cm}^2$, especially the 250 °C treated 0.15 and 0.3 wt % CAN coatings which have an impedance near $1 \times 10^6\ \Omega\text{cm}^2$, corresponding to an improvement of approximately two orders of magnitude over that of the unmodified PS. Because the $|Z|$ values reflect the extent of ionic conductivity generated by the electrolyte passing through the coating layers, a high value of $|Z|$ appears to imply a low degree of penetration of electrolyte into the coating films. Hence, from a comparison of $|Z|$ values, the most effective PS coatings for reducing the rate of penetration of NaCl electrolyte can be prepared by adding 0.15 and 0.3 wt % CAN oxidizing agents at 250 °C, thereby resulting in some degree of protection of aluminium against corrosion.

The information on the EIS was supported by salt-spray resistance tests for all the coated aluminium panels. A trace of rust stain was generally looked for in evaluating the results for salt-sprayed specimens. As shown in Table I, the results were reported as the total exposure time at the date of the generation of the rust stain from the aluminium surfaces. All the unmodified

TABLE I Salt-spray resistance of aluminium substrates coated with CAN-modified and unmodified PS at 150, 200 and 250 °C

CAN (wt %)	Treatment temperature of film (°C)	Salt-spray resistance (h)
0	150	< 24
0	200	< 24
0	250	< 24
0.07	150	< 24
0.07	200	30
0.07	250	48
0.15	150	30
0.15	200	48
0.15	250	168
0.30	150	30
0.30	200	48
0.30	250	168

PS coatings at 150, 200 and 250 °C failed in an exposure period of only 24 h. Although the surface of the 0.07 wt % CAN-modified PS coating at 150 °C was corroded after exposure to the salt fog within 24 h, the increase in treatment temperature of this coating extended the protection to 30 and 48 h at 200 and 250 °C, respectively. By comparison with the 0.07 wt % CAN coatings, an increased amount of CAN at high temperature afforded good protection. In fact, the coatings modified with 0.15 and 0.3 wt % CANs at 250 °C had a salt-spray resistance for 168 h.

Relating this finding to the molecular structure of coatings, it is very interesting to note that the extent of corrosion protection afforded by the PS coating depends primarily on the complexity of the Ce^{4+} salt-bridge carboxylate conformations formed by the oxidation of CAN-modified PS; coating films containing a large number of cerium-complexed carboxylate displayed a better protection of aluminium from the corrosion, than those of a poor complexity and an uncomplexed carboxylate.

3.3. Adhesion

Assuming that these thin complex films in the range of approximately 1.0–2.5 μm are used as primer coatings of aluminium, our attention then focused on their adherence to polymeric top-coatings. In this study, only polyurethane (PU) polymer was applied as elastomeric top-coating material. To gain information on the adherent behaviour of primers, the samples were prepared in the following manner. The surfaces of the alkali-cleaned aluminium substrates were treated with 0.3 wt % CAN-modified and unmodified PS primers, and then heated for 2 h at 150, 200 and 250 °C. PU, ≈ 2 mm thick, was coated over the primed aluminium surfaces, and then cured in an oven at 80 °C. As described in our previous paper [11], the identification of the failure locus occurring at the interfaces of PU topcoat/PS primer/Al substrate joint systems provides information on evaluating the interfacial adhesive performance; namely, the most ideal failure mode is a cohesive one in which the loss of adhesion occurs in the PU layers, thereby developing a great bond strength at interfaces between the primer and PU or

TABLE II Atomic composition (at %) of interfacial aluminium sites removed from PU coatings in PU top-coat/PS Primer/Al substrate joint systems

CAN (wt%)	Temperature (°C)	Al	C	N	O
0	150	7.64	49.21	0.00	43.15
0	200	0.00	72.77	2.08	25.15
0	250	0.00	75.13	2.13	22.73
0.3	150	0.00	72.55	2.95	24.50
0.3	200	0.00	73.77	3.49	22.74
0.3	250	0.00	73.70	3.51	22.79

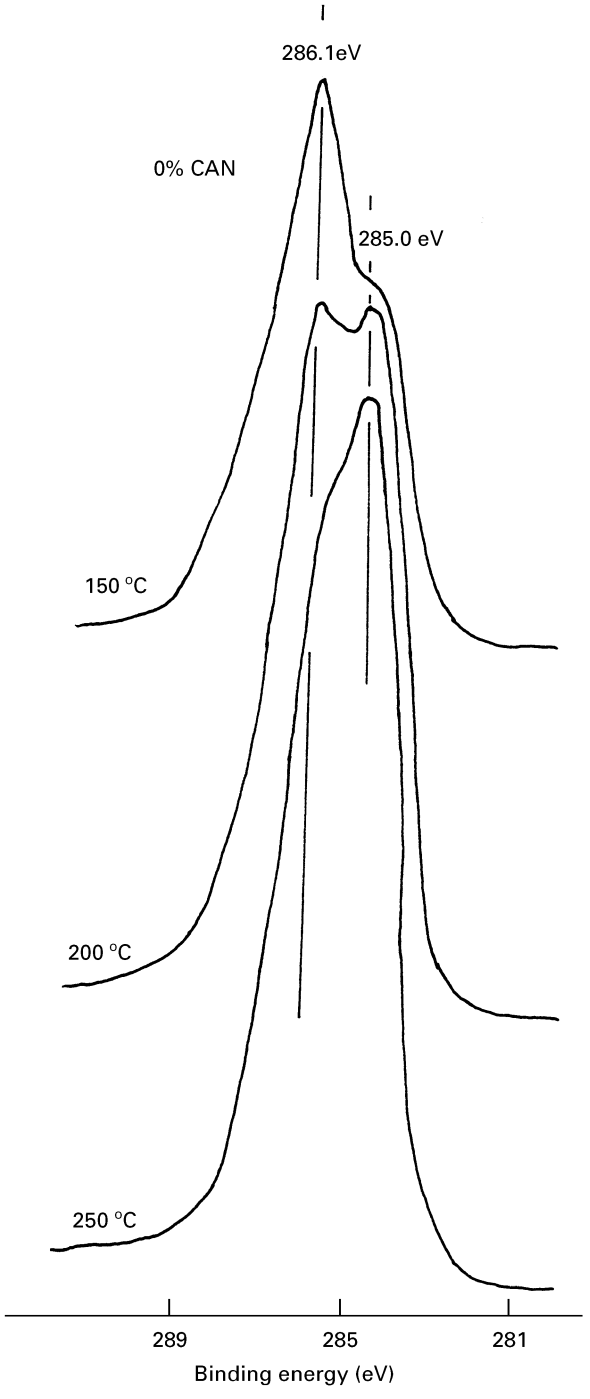

Figure 8 C1s region for interfacial aluminium surfaces removed from PU top-coatings in PU/150, 200, and 250 °C oxidized bulk PS primer/Al joint systems.

aluminium. Thus, the PU coatings adhering to the primer were physically separated from the primed aluminium surfaces. After removing PU, the interfacial aluminium surface sites were examined to identify the locus of bond failure. These data were obtained from a comparison between the XPS peak areas, which were converted into the atomic concentrations by means of the differential cross-sections for core-level excitation of the respective elements. The internally generated Al2p, C1s, N1s and O1s peak areas were used to obtain the atomic per cents. The C1s region also was investigated to substantiate further the mode of failure.

The changes in the XPS atomic composition and the spectral features of the C1s region as function of oxidizing temperature of primers are given in Table II, and in Figs 8 and 9. For the unmodified PS primers denoted as 0 wt % CAN (Table II), the atomic composition of the interfacial aluminium site with a 150 °C treated primer was characterized by having 7.64% aluminium, a large amount of carbon and oxygen, and 0% nitrogen. The sources of aluminium and oxygen elements come from the aluminium oxide layers existing at the outermost surface site of the underlying aluminium substrates [11]. In connection with the presence of carbon, the oxygen can also be associated with the PS primer. The PU has two nitrogen-related groups, isocyanate (–NCO) and urethane ($-NHCO_2$). Thus, the lack of a nitrogen signal seems to suggest that the amount of PU remaining on the primed aluminium after removing PU is very small, if any. In other words, most PU layers were isolated from the primed aluminium surfaces during the failure. Using the 200 °C treated primers, the differences in elemental distribution, compared with that of the 150 °C treated one, were as follows: (1) the presence of a certain amount of nitrogen, (2) a marked increase in the amount of carbon, (3) no aluminium signal, and (4) a pronounced reduction of the oxygen atom. From finding (3), it is conceivable that failure occurs through the coating layers away from the underlying aluminium. This information verified that the primer treated at 200 °C had some chemical affinity with the aluminium surfaces. Such an affinity probably develops a good adhesive force at interfaces between the primer and aluminium. This interfacial bond strength might be greater than those of primer and PU layers. However, there is no evidence whether the disbandment takes place in the primer, PU, or their mixed layers.

Nevertheless, it is apparent that the oxidation of PS in the presence of atmospheric oxygen at 200 °C causes the formation of C=O derivatives. Thus, a possible interpretation for the good bonding behaviour of PS to the aluminium may be due to a high reactivity of the C=O derivative as a functional group with the Al_2O_3 as the top-surface layers of aluminium. At 250 °C, the atomic composition closely resembled that of the aluminium interface at 200 °C.

To support this information, we assessed the chemical states at the BE positions of photoelectron signals which emerged in the C1s region. As seen in Fig. 8, the C1s curve of the 150 °C primed aluminium interfaces

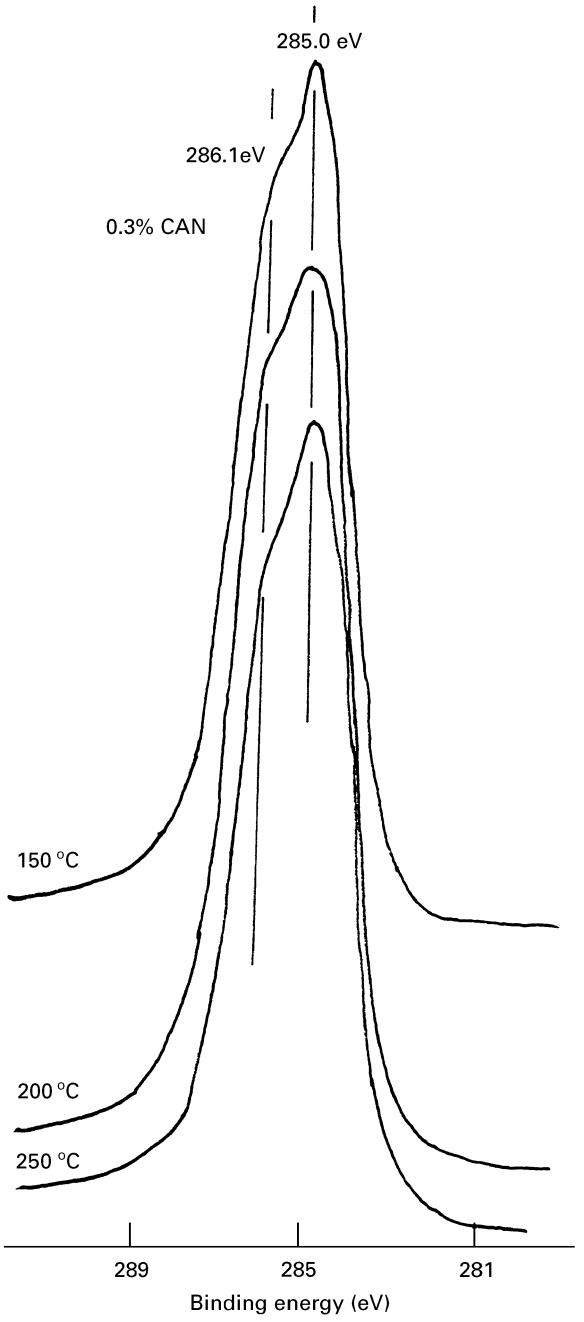

Figure 9 C1s spectra for interfacial aluminium surfaces separated from PU top-coatings in PU/thermally oxidized 0.3 wt % CAN primer/Al joint systems.

separated from the PU showed the excitations of two distinctive peaks at 286.1 and 285.0 eV. The latter shoulder peak, as a minor component, is assignable to the carbon in the $-CH_2-$ compounds. When the contributors to the major carbon peak at 286.1 eV were considered, it is possible that they encompassed the four carbon-related groups, the alcohol and ether carbons in the primer, and the diphenylic carbons joined to oxygen and nitrogen, such as $\equiv C-O-$ and $\equiv C-N=$ in the PU. However, as mentioned in the atomic composition study (Table II), there are no nitrogen atoms originating from the PU. Thus, the carbon peak at 286.1 eV is more likely to be associated with that in the primer, rather than in the PU. Assuming that this interpretation is reasonable, the loss of adhesion is not only due to the cohesive failure through the primer layers adjacent to the underlying aluminium, but also occurs at the interfaces between primer to the aluminium, as adhesive failure. Such a failure mode, which can be described as a mixed mode of cohesive and adhesive ones, suggested that the extent of the adherence of primer to the aluminium is poor, thereby creating a weak primer/metal boundary layer. In other words, the magnitude of the interfacial bonding between the primer and aluminium is lower than that for the PU-to-primer interfacial bond. By comparison with that at 150 °C, the curve from the aluminium interface at 200 °C exhibited a doublet feature in which the peak intensity at 286.1 eV is almost the same as that at 285.0 eV, while the area in the overall curve had grown significantly. Relating this finding to the fact that the interfacial aluminium surfaces have some nitrogen atoms (Table II), it was inferred that the failure may propagate through the PU/primer mixed layers. These data substantially supported the finding that the functional C=O derivative formed by the oxidation of PS at 200 °C enhances its chemical affinity with the Al_2O_3. At 250 °C, a specific feature of the C1s spectrum was that the peaks at 285.0 and 286.1 eV become the principal and shoulder signals, respectively. Although the data are not shown in any of the figures, the C1s region of PU itself showed a spectral feature similar to that taken from the aluminium interface at 250 °C. Hence, the cohesive failure through the PU layers can be proposed as the disbandment mode in this coating system. Such information engendered the interesting concept that the 250 °C treated primer promotes the adherence to both the PU and aluminium sites. Because a further oxidation of C=O derivative at 250 °C converts it into the COO^- derivative, it is believed that the intermediate primer layers, consisting of a mixture of these functional derivatives, perhaps act to link tightly between the PU and aluminium substrate. Also, from this failure mode, the interfacial bond strengths developed at interfaces between primer and aluminium or PU appear to be much stronger than that of the PU itself. As a result, primers containing a large number of oxidation-derived C=O, and COO^- groups contribute significantly to improving the interfacial bonding of both the PU and aluminium sides, reflecting the formation of the most effective intermediate layers as interfacial tailoring.

Returning to Table II, when the 0.3 wt % CAN-modified PS s were applied as primer coatings, the surface chemical composition for all the aluminium interfaces at 150, 200, and 250 °C had a similar elemental distribution; there was no aluminium, 72.55%–73.70% C, 2.95%–3.51% N, and 24.50%–22.79% O. As is evident from the absence of aluminium, disbandment is generated in the coating layers. In support of this information, a comparison between the C1s spectral features taken from these interfacial samples is shown in Fig. 9. As expected, all the spectra showed the PU-related curve feature, implying that the loss of adhesion occurs in the PU layers as the mode of cohesive failure. Relating this finding to the IR and XPS data, the major chemical factor of the primer

contributing to a high adhesive performance was due to the incorporation of functional C=O and cerium-complexed carboxylate derivatives into the PS by CAN-catalysed oxidation, followed by thermal oxidation in air at high temperature.

4. Conclusion

In the oxidation of potato-starch (PS) polymers, the conversion of PS colloidal solutions containing cerium (IV) ammonium nitrate (CAN) as an oxidizing agent into solid states by heating in the presence of atmospheric oxygen at 150 °C introduced functional C=O derivatives formed by the cleavage of glycol C–C bonds in the glycosidic rings in terms of ring openings. Progressive oxidation of CAN-modified PS by thermal treatments at 200 and 300 °C not only resulted in the incorporation of oxygen into the C=O derivatives, but also caused the breakage of C–O–C linkages in the open rings. Such a highly oxidizing process led to the generation of intermediate carboxylate (COO^-) derivatives which finally transformed into cerium-bridged carboxylate complexes formed by reactions between the Ce^{4+} released from CAN and the COO^-.

When such an oxidized PS film is applied as the primer coating of aluminium substrates, the following generalizations can be made about the specific characteristics of this primer. (1) the ranking of oxidation-induced functional derivatives in reducing the ionic conductivity generated by NaCl electrolyte passing through the film layers, was in the order of cerium-complexed carboxylate > carboxylate > carbonyl > unoxidized PS, suggesting that the complexed carboxylate films displayed a far better protection of aluminium against corrosion, than did unoxidized PS films, and (2) in the adherence aspect of intermediate primer layers to both polyurethane (PU) top-coat and aluminium substrate sites, all the functional derivatives contributed significantly to improving the adhesive bonding which links tightly between the PU and aluminium, thereby resulting in the cohesive failure in which the loss of adhesion occurs in the PU layers.

Accordingly, the oxidation of environmentally benign nature polymers is a very attractive process for fabricating intermediate primer films which afford some degree of protection of aluminium from corrosion, and ensure the development of a strongly linked boundary layer.

Acknowledgements

This work was performed under the auspices of the US Department of Energy, Washington, DC under Contract DE-AC02-76CH00016, and supported by the US Army Research Office Program MIPR-96-40.

References

1. J. M. WINTON, M. HOZEL, J. CAMPBELL, C. EHRLE, J. R. HART, L. LAZORHO and K. PORTNOY, *Chemical Week* **14** (1987) 30.
2. F. W. SCHNCK and R. E. HEBEDA, "Starch Hydrolysis Products" (VCH, New York, 1992) p. 32.
3. T. SUGAMA, *Mater. Lett.* **25** (1996) 291.
4. R. MEHROTRA and B. RANBY, *J. Appl. Polym. Sci.* **21** (1977) 1647.
5. T. DOBA, C. RODEHED and B. RANDY, *Macromolecule* **17** (1984) 2512.
6. J. P. GAO, R. C. TIAN, J. G. YU and M. L. DUAN, *J. Appl. Polym. Sci.* **53** (1994) 1091.
7. L. J. BELLAMY, "The Infra-red Spectra of Complex Molecules" (Chapman and Hall, London, 1975) p. 183.
8. D. BRIGGS and M. P. SEAH, "Practical Surface Analysis by Auger and X-ray Photoelectron Spectroscopy" (Wiley, New York, 1984) p. 385.
9. J. W. BARTHA, P. O. HAHN, F. LEGOUES and P. S. HO, *J. Vac. Sci. Technol.* **3** (1985) 1390.
10. J. F. MOULDER, W. F. STICKLE, P. E. SOBOL and K. D. BOMBEN, "Handbook of X-ray Photoelectron Spectroscopy" (Perkin-Elmer Corporation, Minnesota, 1992) p. 218.
11. T. SUGAMA, L. E. KUKACKA and N. CARCIELLO, *Int. J. Adhes. Adhesives* **8** (1988) 101.

Received 23 July
and accepted 23 October 1996